Heavy flavor production in STAR

Daniel Kikoła[1] for the STAR Collaboration
Purdue University, West Lafayette, IN, US
E-mail: kikola@if.pw.edu.pl

Abstract.
We report on the recent STAR results on heavy flavor production in Au+Au collisions at $\sqrt{s_{NN}} = 200$, 62.4 and 39 GeV. We present the nuclear modification factor and elliptic flow of open charm mesons and electrons from semileptonic decays of heavy flavor hadrons. We also report on new measurements of energy dependence of J/ψ production. STAR data are compared to theoretical model calculations and physics implications are discussed.

1. Introduction

Heavy quarks, charm and bottom, are unique probes of the Quark Gluon Plasma (QGP) properties at RHIC because they are produced in the initial interactions with large momentum transfer, before the QGP phase, and they are expected to interact with the QGP differently from light quarks. Experimentally, we study heavy quark production via decay products of charmed and beauty hadrons. At the moment, there are two feasible techniques for such studies at RHIC: using electrons from semi-leptonic decay of open heavy flavor mesons (so called non-photonic electrons, NPE), or through hadronic decays of charmed mesons. In the first case, the yields are larger and a specialized trigger can be used, although the information about the parent meson kinematics is incomplete and such an electron sample is a mixture of electrons from charmed and beauty hadron decays. In the latter, we identify charmed mesons via hadronic decays (e.g. $D^0 \to K^-\pi^+$) which give access to the kinematic of parent meson, but it suffers from large combinatorial background if a vertex detector is not available.

Elliptic flow of heavy quarks is another important tool for studying the QGP properties. It can shed new light on possible collective behavior and degree of thermalization of nuclear matter created in heavy ion collisions. Simultaneous measurements of the c and b quark production and elliptic flow are crucial for understanding the nature of interactions of heavy quarks with the surrounding partonic medium, and the parton energy loss mechanism in general.

Measurements of the production of various quarkonia states can provide insight into thermodynamic properties of the QGP. Different states have different binding energy and therefore disassociate, due to the Debye screening of the quark-antiquark potential, at different temperatures. However, there are other effects that may affect the observed production, such as cold nuclear matter effects, final state nuclear absorption and statistical coalescence of quark-antiquark pairs. The study of quarkonia production for different colliding systems, collision energies and centralities can help to disentangle the interplay of these mechanisms and to understand the medium properties.

[1] Present address: Faculty of Physics, Warsaw University of Technology, Warsaw, Poland

Besides studies of the QGP properties at top RHIC energy, we measure heavy quark production as a function of colliding energy in RHIC Beam Energy Scan program. Such measurements, complementary to the results for light quarks, provide us with additional means to map out the phase diagram of nuclear matter.

2. Data analysis

STAR [1] is a large acceptance ($|\eta|$ <1, full coverage in ϕ) multipurpose detector composed of several subsystems, which is well suited for the measurement of heavy quark production. In the analyses reported here, STAR Time Projection Chamber (TPC), Barrel Electromagnetic Calorimeter (BEMC) and Time-Of-Flight (TOF) detectors are used. We reconstruct quarkonia (J/ψ, Υ) via the di-electron decay channel. We identify charmed mesons via their hadronic decays (e.g. $D^0 \rightarrow K^-\pi^+$). The TPC is used for charged track reconstruction and particle identification via specific ionization energy loss (dE/dx). BEMC is used at high p_T for electron selection and also for a high-p_T (p_T > 2 GeV) electron trigger, while TOF provides electron identification at low p_T. For direct reconstruction of open charm mesons, TOF information together with the dE/dx are combined to select daughter pion and kaon candidates. In this article, we present results obtained with Au+Au data collected in 2010 and 2011 at $\sqrt{s_{\rm NN}} = 200$, 62 and 39 GeV and $p+p$ $\sqrt{s} = 200$ GeV data taken in 2009. More details about NPE and charmed meson measurements at STAR can be found in Refs. [2, 3, 4].

3. Results

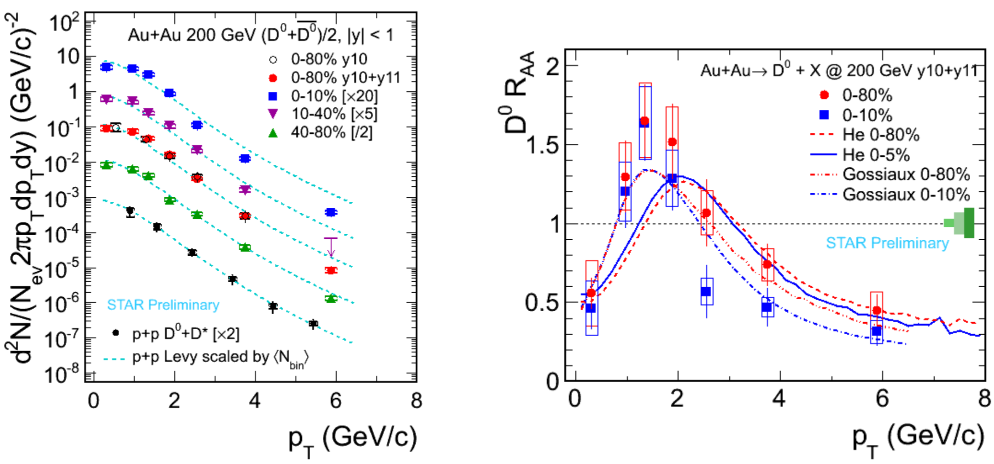

Figure 1. Left panel: D^0 invariant yield as a function of p_T in $p+p$ and Au+Au collisions at $\sqrt{s_{\rm NN}} = 200$ GeV. The dashed lines represent a Levi fit to $p+p$ data scaled by the number of binary collisions in a given centrality bin. Right panel: D^0 nuclear modification factor as a function of p_T in central (0-10%) and min-bias (0-80%) Au+Au collisions. The lines represent model calculations by He et al. [5] and Gossiaux et al. [6].

The left panel of Fig. 1 shows D^0 p_T spectrum in $p+p$ and Au+Au collisions at $\sqrt{s_{\rm NN}} = 200$ GeV. The dashed lines represent a Levi fit to $p+p$ data scaled by the number of binary collisions ($N_{\rm bin}$) in a given centrality bin. The Levi fit describes the $p+p$ data well; however, there are clear discrepancies when the fit is compared to Au+Au data. To quantify a modification of the D^0 production in Au+Au collisions, we calculate the nuclear modification factor R_{AA}: $R_{AA} = \frac{{\rm d}^2N_{Au+Au}/dydp_T}{N_{\rm bin}\times {\rm d}^2N_{p+p}/dydp_T}$, where ${\rm d}^2N_{Au+Au}/dydp_T$ and ${\rm d}^2N_{p+p}/dydp_T$ are invariant yields in Au+Au and p+p collisions, respectively, and $N_{\rm bin}$ is the number of binary collisions in a given Au+Au centrality class. The right panel of Fig. 1 shows the D^0 R_{AA} for 0-10% most central and minimum bias Au+Au collusions. At high p_T, D^0 production is significantly suppressed. Moreover, D^0 production is enhanced at intermediate p_T (a "bump" at $p_T \sim 1.5$ GeV/c). The STAR data are compared to model predictions by He et al. [5] and Gossiaux et al. [6]. Both models assume that heavy quarks are strongly coupled with the surrounding partonic medium and predict a large suppression at high p_T. The models qualitatively reproduce the shape of R_{AA} as a function of p_T. The enhancement at $p_T \sim 1.5$ GeV/c in those calculations is due to the charm quark and medium interaction as well as the radial flow of light quarks which coalesce with charm quarks to produce D mesons. However, a similar effect for other particles (protons, pions) is observed at intermediate p_T in d+Au collisions [7] (the Cronin effect).

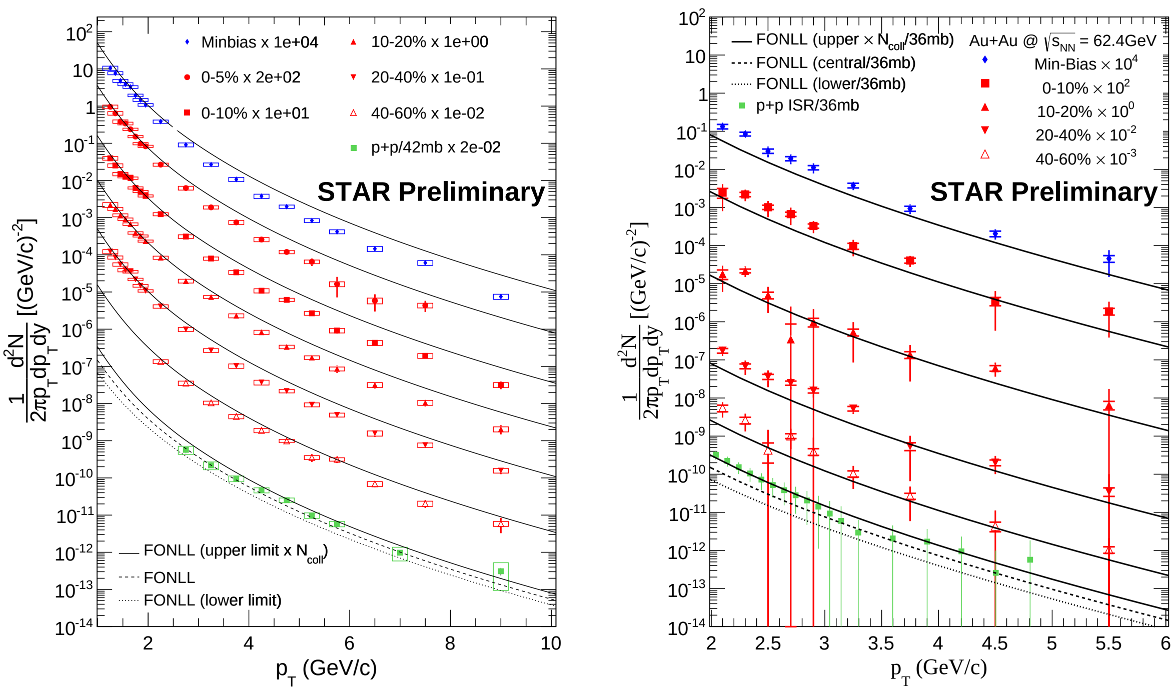

Figure 2. Invariant yield of non-photonic electrons as a function of p_T in Au+Au collisions at $\sqrt{s_{\rm NN}} = 200$ GeV (left panel) and at $\sqrt{s_{\rm NN}} = 62$ GeV (right panel). Solid lines represent an upper limit on FONLL predictions for NPE production scaled by number of binary collisions ($N_{\rm bin}$) in a given centrality. For 62 GeV, ISR results for NPE p_T spectrum [8] are also presented.

Figure 2 shows the NPE p_T spectra for Au+Au collisions at $\sqrt{s_{\rm NN}} = 200$ and 62.4 GeV. The data are compared with FONLL calculations scaled by $N_{\rm bin}$ corresponding to a given centrality bin. At 200 GeV, NPE production in central and mid-central collisions is suppressed compared to FONLL; however, the suppression is not observed at 62.4 GeV. Note, that results for 62.4 GeV are not corrected for $J/\psi \to e^+e^-$ contribution, which is as large as $\sim 20\%$ at high p_T at 200 GeV. Figure 3 shows the $R_{\rm AA}$ and elliptic flow of non-photonic electrons. We observe a strong NPE suppression at high p_T in central collisions, similar to D^0 and light hadrons ($\pi^{\pm}$). Figure 3 (right panel) shows v_2 results obtained using two- and four-particle correlations ($v_2\{2\}$ and $v_2\{4\}$, respectively). $v_2\{2\}$ and $v_2\{4\}$ have different sensitivity to the flow fluctuations and so called nonflow (correlations not related to the reaction plane) and thus provide an upper and lower limit on the average elliptic flow [9]. We compare our data to a few model calculations.

The DGLV model with radiative energy loss only [10] underestimates the observed suppression; however, it gives a reasonable description of the data when collisional energy loss is added. The collisional dissociation model [11] and AdS/CFT correspondence calculations [12] can also describe the measured R_{AA} reasonably well. In a partonic transport model, BAMPS [13, 14], heavy quarks lose energy due to elastic collisions with the rest of the medium. The dashed-dotted green line shows predictions for v_2 from the implementation of radiative and collisional energy loss from Gossiaux et al. [15, 6]. He et al. employ the TMatrix interactions model [5] which is a non-perturbative approach to heavy quark energy loss. Each of these models predicts a non-zero v_2 of charm quarks, thus observed finite NPE v_2 suggest a finite elliptic flow of charm quarks which is acquired due to interactions with quarks and gluons in the QGP phase. At 200 GeV, v_2 increases with p_T for $p_T > 3$ GeV which is likely due to decay or jet-like correlations.

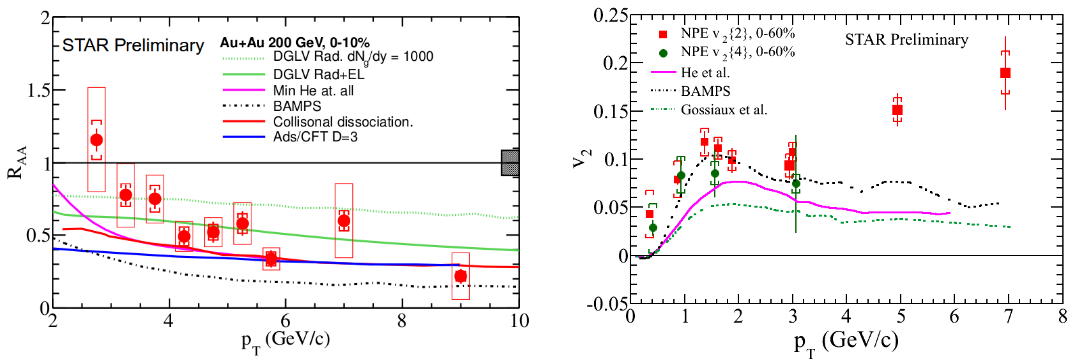

Figure 3. Non-photonic electron nuclear modification factor (left panel) and elliptic flow (v_2) (right panel) at $\sqrt{s_{\rm NN}} = 200$ GeV.

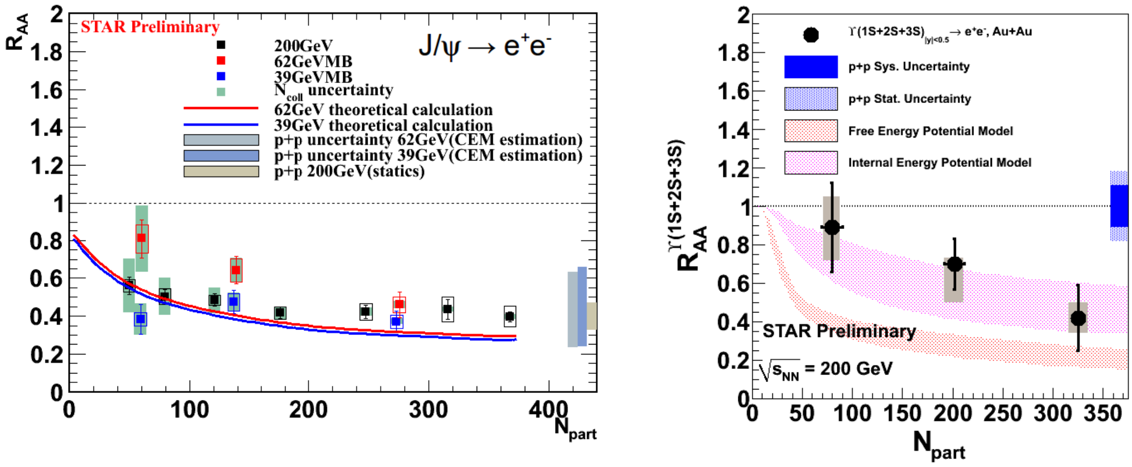

Figure 4. Left panel: nuclear modification factor $R_{\rm AA}$ for low$-p_T$ ($p_T < 5$) GeV/c J/ψ at $\sqrt{s_{\rm NN}} = 200$, 62.4 and 39 GeV. Right panel: $R_{\rm AA}$ for Υ at top RHIC energy.

The left panel of Fig. 4 shows the nuclear modification factor as a function of centrality (represented by number of participants, $N_{\rm part}$) for low$-p_T$ ($p_T < 5$) GeV/c J/ψ in Au+Au collisions at $\sqrt{s_{\rm NN}} = 200$, 62.4 and 39 GeV. In the case of 39 and 62 GeV, predictions of the Color Evaporation Model [16] are used as a baseline, with uncertainties indicated by boxes on the right hand side of the plot. We observe a significant suppression at 39 and 62 GeV, at the similar level to $\sqrt{s_{\rm NN}} = 200$ GeV. STAR data are compared to predictions from model by Zhao and Rapp [17] which assumes two main components: suppression of directly produced J/ψ due to color screening and secondary production via recombination of $c, \bar{c}$ quarks. The model predicts very similar suppression for both 39 and 62 GeV, despite the significant difference in energy and thus different initial energy densities. In this model, larger direct suppression at higher energy is compensated by an enhanced regeneration rate due to the larger cross section for charm quarks. These calculations agree reasonably well with our data within errors.

The right panel of Fig. 4 shows the nuclear modification factor as a function of centrality for Υ in Au+Au collisions at $\sqrt{s_{\rm NN}} = 200$ GeV. The suppression increases with centrality and a significant suppression is observed in the most central collisions. Data are compared to a model by Strickland et al. [18], which assumes a thermal dissociation of Υ in a thermalized, expanding partonic medium, simulated with relativistic hydrodynamics. These calculations predict almost complete suppression of $\Upsilon(2S)$ and $\Upsilon(3S)$ states in the most central collisions. The model reproduces the STAR results well and the data favors the internal energy potential scenario.

4. Summary

D^0 and non-photonic electron production are suppressed at high p_T in Au+Au collision at $\sqrt{s_{\rm NN}} = 200$ GeV. On the other hand, NPE spectra at $\sqrt{s_{\rm NN}} = 62.4$ GeV is not suppressed compared to the pQCD calculations. We also observe a finite elliptic flow of non-photonic electrons $\sqrt{s_{\rm NN}} = 200$ GeV and comparison with models suggests a finite elliptic flow of charm quarks. J/ψ suppression at lower energies (39 and 62 GeV) is similar to top RHIC energy. The Υ suppression at $\sqrt{s_{\rm NN}} = 200$ GeV increases with centrality and it is consistent with a model that assume complete suppression of $\Upsilon(2S)$ and $\Upsilon(3S)$ states.

References

[1] Anderson M *et al.* 2003 *Nucl. Instrum. Meth. A* **499** 659–678 (*Preprint* nucl-ex/0301015)
[2] Agakishiev H *et al.* (STAR Collaboration) 2011 *Phys. Rev. D* **83** 052006 (*Preprint* 1102.2611)
[3] Tlusty D (STAR collaboration) 2013 *Nucl. Phys. A 904-905* **2013** 639c–642c (*Preprint* 1211.5995)
[4] Mustafa M (STAR Collaboration) 2013 *Nucl. Phys. A 904-905* **2013** 665c–668c (*Preprint* 1210.5199)
[5] He M, Fries R J and Rapp R 2012 *Phys. Rev. C* **86** 014903 (*Preprint* 1106.6006)
[6] Gossiaux P, Aichelin J, Gousset T and Guiho V 2010 *J. Phys. G* **37** 094019 (*Preprint* 1001.4166)
[7] Adare A *et al.* (PHENIX Collaboration) 2013 (*Preprint* 1304.3410)
[8] Basile M *et al.* 1981 *Il Nuovo Cimento A* **65** 421–456 ISSN 0369-3546
[9] Voloshin S A, Poskanzer A M, Tang A and Wang G 2008 *Phys. Lett. B* **659** 537–541 (*Preprint* 0708.0800)
[10] Djordjevic M, Gyulassy M, Vogt R and Wicks S 2006 *Phys. Lett. B* **632** 81 – 86
[11] Sharma R, Vitev I and Zhang B W 2009 *Phys. Rev. C* **80**(5) 054902
[12] Horowitz W 2008 *J. Phys. G* **35** 044025 (*Preprint* 0710.0703)
[13] Uphoff J, Fochler O, Xu Z and Greiner C 2011 *Phys. Rev. C* **84** 024908 (*Preprint* 1104.2295)
[14] Uphoff J, Fochler O, Xu Z and Greiner C 2012 *Phys. Lett. B* **717** 430–435 (*Preprint* 1205.4945)
[15] Gossiaux P and Aichelin J 2008 *Phys. Rev. C* **78** 014904 (*Preprint* 0802.2525)
[16] Nelson R E, Vogt R and Frawley A D 2013 *Phys. Rev. C* **87**(1) 014908 (and private communication)
[17] Zhao X and Rapp R 2010 *Phys. Rev. C* **82** 064905 (and private communication) (*Preprint* 1008.5328)
[18] Strickland M 2011 *Phys. Rev. Lett.* **107** 132301 (*Preprint* 1106.2571)